Parameter Extraction For Quantum Well DFB Lasers Based on 1D Traveling Wave Model

Jiewen Chi, Chuanning Niu, and Jia Zhao

***Abstract*—Extracting the parameters of a laser from the measured results is critical for laser design, modeling and optimization. This work presents a parameter extraction method for quantum well distributed feedback (DFB) lasers based on the one-dimensional traveling wave model (1D TWM). Facet reflectivities, grating coupling coefficient and the other parameters can be extracted by fitting the lasing spectrum, light-current (L-I) curve, intensity modulation (IM) response and large-signal chirp. During the extraction progress, the 1D TWM is simplified to improve the extraction efficiency. The feasibility of this extraction method is verified by extracting parameters from preset simulation results and experimental results, respectively. The 1D TWM can reflect the physical properties of the laser profoundly and the parameter extraction method based on 1D TWM will be a valuable tool for laser design, optimization or processing improvement.**

***Index Terms*—DFB lasers, parameter extraction, 1D TWM, rate equation.**

I. Introduction

QUANTUM well distributed feedback (DFB) lasers are important light sources for high-speed optical communication systems owing to the advantages of large differential gain, low threshold current, wide direct modulation bandwidth and narrow linewidth [1], [2], [3]. To fulfill the growing demands of directly modulated DFB lasers, great effort has been put into improving the modulation bandwidth, single longitudinal mode stability, and emission efficiency for a long time [4], [5].

Parameters, such as the cavity length, facet reflectivities, grating coupling coefficient and differential gain coefficient, determine the output properties of a laser, including the lasing spectrum, light-current (L-I) curve, intensity modulation (IM) response and so on. To put it another way, the output characteristics of the laser can be predicted through simulation with a set of already known parameters, which is an important step in laser design. Extracting the related simulation parameters from the measured results is also an important part in the laser modeling and simulation process. On the one hand, the accurate simulation parameters can ensure that the simulation results match the experimental results. On the other hand, it can reflect the differences between the actual and the design parameters of a laser, which can guide us to optimize the laser design and improve the laser processing.

The rate equation model and the one-dimensional traveling wave model (1D TWM) are the most common methods in the simulation of semiconductor lasers, according to a large amount of research on the modeling of semiconductor lasers [6], [7], [8], [9], [10], [11], [12], [13]. The parameter extraction methods based on the rate equation model, have gotten a lot of attention due to the simplicity and quick simulation speed of the rate equation model, which provide a helpful tool for laser design [14], [15], [16], [17], [18], [19], [20]. However, the rate equation model is a zero-dimensional approximation of the 1D TWM. It does not contain any structure information along the cavity such as grating period and grating coupling coefficient. Effects like longitudinal spatial hole burning (LSHB) and forward- and backward-going waves coupling caused by the grating are ignored. The rate equation model is suitable for simulating Fabry-Perot (FP) lasers with no grating along the cavity. While for DFB lasers, the 1D TWM is more appropriate and the parameters extracted based on 1D TWM are more accurate. Although the 1D TWM can better reflect the physical features of a laser, only a limited amount of work has been done on parameter extraction using 1D TWM because of its complexity. Among these work, most of them are focus on the extraction of single or several parameters [21], [22].

In this paper, the parameter extraction method for DFB lasers based on 1D TWM is presented. Almost all parameters of the laser involved in the 1D TWM can be extracted by fitting the laser's output characteristics, including the L-I curve, lasing spectrum, large-signal chirp and IM response [23]. Given the complexity of 1D TWM in comparison to the rate equation model, the normalized rate equation model and the analytical expressions of effective parameters are obtained by simplifying the 1D TWM. The value ranges of the 1D TWM parameters can be determined according to the obtained values of the effective parameters. The determined value ranges are helpful to accelerate parameter extraction progress. We firstly apply the method to extract the laser's parameters from preset simulation results. The extracted parameters are quite near to the preset parameters and the simulation results using the extracted parameters are in good agreement with the preset results. The method is then used in experimental results extraction, and the simulated results using the extracted parameters match the actual results quite closely.

The organization of this paper is as follows. The derivation of related formulae and the specific process of parameter extraction

Manuscript received 20 June 2022; revised 16 August 2022; accepted 22 August 2022. Date of publication 31 August 2022; date of current version 6 September 2022. This work was supported by the National Key Research and Development Programs of China under Grant 2018YFA0209001. (*Corresponding authors: Chuanning Niu; Jia Zhao.*)

The authors are with the School of Information Science and Engineering, Shandong University, Qingdao 266237, China (e-mail: chijiewen@mail.sdu.edu.cn; niuchuanning@sdu.edu.cn; zhaojia@sdu.edu.cn).

Digital Object Identifier 10.1109/JPHOT.2022.3201578

are described in Section II. In Section III, the extraction method described in Section II is applied to extract parameters from preset simulation results and experimental results, respectively. Finally, the overall conclusions are stated in Section IV.

II. Parameter Extraction Process

The output characteristics of the laser include L-I curve, lasing spectrum, IM response and large-signal chirp, etc. A laser's output characteristics are determined by its physical or quasi-physical parameters. In this paper, we refer to the parameters, such as cavity length, grating period, active region volume and facet reflectivities, which directly related to the physical structure of the laser as physical parameters. The parameters, such as grating coupling coefficient, effective index without injection, differential gain coefficient, transparent carrier density, nonlinear gain saturation coefficient, carrier lifetime, internal loss, linewidth enhancement factor and optical confinement factor, which are determined by the physical structure and materials but need to be calculated are defined as quasi-physical parameters. This chapter introduces a method for extracting these parameters of a DFB laser through its output characteristics.

A. Parameter Extraction Via Lasing Spectrum

The lasing spectrum of a DFB laser is related to its cavity length, grating period, grating coupling coefficient, effective index and facet reflectivities [24]. When the above parameters are known, the lasing spectrum can be determined. Transfer matrix method (TMM) is the most commonly utilized approach to simulate the lasing spectrum [25]. The structural parameters of the laser, including the grating period, cavity length and active region volume, can all be obtained by cutting the laser. Therefore, the above structure parameters are known in the process of parameter extraction. With the given lasing spectrum, the effective index without injection, grating coupling coefficient and facet reflectivities can be extracted preliminarily. The following are the precise extraction steps:

a) Using established parameters for the cavity length and grating period;
b) Assigning initial values to the effective index without injection, grating coupling coefficient and facet reflectivities (the amplitude reflectivity of front facet r_f and back facet r_r);
c) Calculating the lasing spectrum using the TMM;
d) Constructing the error function between the calculated and the known lasing spectra;
e) Determining the final values of effective index without injection, grating coupling coefficient and facet reflectivities by adjusting these three variables to minimize the value of error function. The adaptive differential evolution algorithm is the most prevalent method for minimizing the error function value [26], [27], [28].

The effective index is expressed as $n_{eff} = n_{eff}^0 - \Gamma\alpha_{LEF}g_{op}\lambda_0/4\pi$ in 1D TWM. It can be seen from the above expression that the effective index is related to the no injection effective index n_{eff}^0, the optical confinement factor Γ, the linewidth enhancement factor α_{LEF}, the gain at operation g_{op} and the reference wavelength λ_0. It's worth noting that the gain at operation and the internal loss are linked [29]. When extracting the effective index without injection, the linewidth enhancement factor and the gain at operation according to the lasing spectrum, the problem of multiple solutions will arise. The impact of linewidth enhancement factor on effective index is temporarily ignored in this stage to prevent the appearance of multiple solutions from bringing uncertainty into the following parameter extraction process, which means that we set $\alpha_{LEF} = 0$ in this step. The linewidth enhancement factor will be extracted by the large-signal chirp of the 1D TWM, and the effective index without injection will be modified at the same time. The internal loss will be obtained by fitting the L-I curve and IM response of the 1D TWM.

B. Effective Parameter Extraction Based on Normalized Rate Equations

For 1D TWM-based parameter extraction, if the value ranges are too small, the fitting results will be inaccurate, and if the value ranges are too large, the extraction progress will be too slow. In this section, the 1D TWM will be simplified to a normalized rate equation model. The values of the effective parameters involved in the normalized rate equation model will be obtained from the slope efficiency and threshold current of the L-I curve and the relaxation oscillation frequency and quality factor of the IM response. The values of the effective parameters are helpful to determine the value ranges of the 1D TWM parameters. In the 1D TWM parameter extraction, the determined value ranges can accelerate parameter extraction progress while ensuring the fitting accuracy.

1) Normalized Rate Equations: The 1D TWM of the quantum well DFB semiconductor laser is expressed as:

$$\frac{dN(z,t)}{dt} = \frac{\eta I(t)}{eV} - \frac{N(z,t)}{\tau_n} - \frac{v_g P_s(z,t)\, g(z,t)}{1+\varepsilon P_s(z,t)}, \tag{1}$$

$$\left(\frac{1}{v_g}\frac{\partial}{\partial t}+\frac{\partial}{\partial z}\right)F(z,t) = \left\{-j\delta + \frac{1}{2}\left[\frac{\Gamma g(z,t)}{1+\varepsilon P_s(z,t)} - \alpha\right]\right\} \cdot F(z,t) + j\kappa R(z,t) + \tilde{s}^f(z,t), \tag{2}$$

$$\left(\frac{1}{v_g}\frac{\partial}{\partial t}-\frac{\partial}{\partial z}\right)R(z,t) = \left\{-j\delta + \frac{1}{2}\left[\frac{\Gamma g(z,t)}{1+\varepsilon P_s(z,t)} - \alpha\right]\right\} \cdot R(z,t) + j\kappa F(z,t) + \tilde{s}^r(z,t), \tag{3}$$

where N is the carrier density, η is the current injection efficiency, I is the injected current, e is the electron charge, V is the active region volume, τ_n is the carrier lifetime, $v_g = c/n_g$ is the group velocity, c is the speed of light, n_g is the group index, P_s is the photon density distribution, g is the material optical gain, ε is the nonlinear gain saturation coefficient, j is the imaginary unit, δ is the phase detuning factor from the Bragg wavelength, α is the internal loss, and κ is the grating coupling coefficient. F and R are the forward and backward traveling optical fields in the cavity. $\tilde{s}^f$ and $\tilde{s}^r$ denote the spontaneous emission noises. Among them, P_s can be expressed as $P_s(z,t) = n_{eff}/(2hv_0)\sqrt{\varepsilon_0/\mu_0}\Gamma/(dwv_g)\cdot[|F(z,t)|^2 + |R(z,t)|^2]$, where h is the Planck's constant, v_0 is

the optical frequency corresponding to λ_0, ε_0 is the permittivity of a vacuum, μ_0 is the permeability of a vacuum, d is the thickness of active region, w is the width of active region. g can be expressed as $g\,(z,t) = g_N\,\ln[N(z,t)/N_{tr}]$, where g_N is the differential gain coefficient, N_{tr} is the transparent carrier density. δ can be expressed as $\delta = (2\pi n_{eff}^0)/\lambda_0 - 1/(2\alpha_{LEF}\Gamma g(z,t)) - \pi/\Lambda$, where Λ is the Bragg grating period.

A simplified rate equation model can be derived from the abovementioned 1D TWM:

$$\frac{dS}{dt} = \left(v_g\Gamma g - \frac{1}{\tau_p}\right) S + \gamma\Gamma v_g n_{sp} g, \tag{4}$$

$$\frac{dN}{dt} = \frac{\eta I}{eV} - \frac{N}{\tau_n} - \frac{\Gamma v_g g S}{V}, \tag{5}$$

$$g = \frac{g_N ln\left(\frac{N}{N_{tr}}\right)}{\left(1+\frac{\varepsilon\Gamma S}{V}\right)}, \tag{6}$$

$$P_f = \frac{0.5\left(1-r_f^2\right) v_g \hbar\omega S}{L}, \tag{7}$$

where S is the photon number, τ_p is the photon lifetime, γ is the Petermann factor, n_{sp} is the population inversion factor, N is the carrier density, P_f is the forward output power, r_f is the amplitude reflectivity of front facet, and L is the cavity length.

2) DC Analysis: Neglecting the influence of nonlinear gain saturation effect and spontaneous emission noise at DC, the above rate equation set degenerates into:

$$\left(v_g\Gamma g - \frac{1}{\tau_p}\right) P_f = 0, \tag{8}$$

$$\frac{\eta I}{e} - \frac{NV}{\tau_n} - \frac{2\Gamma g L}{\left(1-r_f^2\right)\hbar\omega} P_f = 0, \tag{9}$$

$$g \approx g_N ln\left(\frac{N}{N_{tr}}\right) = g_N\, ln\left(\frac{NV}{N_{tr}V}\right). \tag{10}$$

Since the spontaneous noise has been ignored, for the forward output power in (8) to be a non-zero finite value, there must be:

$$v_g\Gamma g \approx \frac{1}{\tau_p}. \tag{11}$$

This leads to the solution that:

$$N \approx N_{tr} e^{\frac{1}{v_g\Gamma g_N \tau_p}}. \tag{12}$$

In (9), because the output power is zero at the threshold current (spontaneous emission noise has been neglected), we have:

$$I_{th} \approx \frac{eV}{\eta\tau_n} N \approx \frac{eV}{\eta\tau_n} N_{tr} e^{\frac{1}{v_g\Gamma g_N \tau_p}}. \tag{13}$$

By using (13), (9) can be sorted into:

$$\frac{P_f}{I - I_{th}} = \frac{\eta\hbar\omega\left(1-r_f^2\right) v_g \tau_p}{2eL}. \tag{14}$$

The relationship of the parameters on the right side of (13) and (14) can be obtained according to the threshold current and slope efficiency.

3) AC Analysis: By making small signal assumption and performing Fourier transform, the small signal modulation response can be solved as follows:

$$S_{21} = \frac{\omega_r^2}{(j\omega)^2 + (j\omega)\frac{\omega_r}{Q} + \omega_r^2}, \tag{15}$$

$$\omega_r = \sqrt{\frac{\eta v_g \Gamma}{V} \frac{g_N}{N_{tr} e^{\frac{1}{v_g\Gamma g_N\tau_p}}} \frac{(I - I_{th})}{e}}, \tag{16}$$

$$\frac{1}{Q} = \frac{\varepsilon\omega_r}{v_g \frac{g_N}{N_{tr} e^{\frac{1}{v_g\Gamma g_N\tau_p}}}} + \tau_p\omega_r + \frac{1}{\tau_n\omega_r}, \tag{17}$$

where ω_r is the relaxation oscillation frequency, Q is the quality factor. The detailed derivation can be found in Appendix.

The relationship of the parameters on the right of (16) and (17) can be obtained according to the relaxation oscillation frequencies and the quality factors at different bias currents.

4) Effective Parameter Extraction Process: The extraction process of the effective parameters based on normalized rate equations can be concluded as follows:

a) Setting the cavity length L, the amplitude reflectivity of front facet r_f and the reference wavelength λ_0. The carrier lifetime τ_n is given an initial value in a reasonable range;
b) Obtaining the photon lifetime τ_p by (14);
c) Obtaining Γg_N and $\mathrm{V}N_{tr}$ by (13) and (16) at the same bias current simultaneously;
d) Obtaining $\Gamma\varepsilon/V$ from (17) at a different bias current from step (c);
e) Obtaining a more accurate carrier lifetime τ_n from (17) by known Γg_N, $\mathrm{V}N_{tr}$, $\Gamma\varepsilon/V$, as well as the relaxation oscillation frequency ω_r and the quality factor Q at the same bias current as in step (c);
f) Repeating (a)-(e) until the parameters are stable.

The parameters in the following normalized rate equations can be obtained.

$$\frac{dS}{dt} = \left(v_g\Gamma g - \frac{1}{\tau_p}\right) S + \gamma\Gamma v_g n_{sp} g$$

$$\rightarrow \frac{dS}{dt} = \left(v_g\bar{g} - \frac{1}{\tau_p}\right) S + v_g\gamma n_{sp}\bar{g}, \tag{18}$$

$$\frac{dN}{dt} = \frac{\eta I}{eV} - \frac{N}{\tau_n} - \frac{\Gamma v_g g S}{V}$$

$$\rightarrow \frac{d\bar{N}}{dt} = \frac{\eta I}{e} - \frac{\bar{N}}{\tau_n} - v_g\bar{g}S, \tag{19}$$

$$g = \frac{g_N ln\left(\frac{N}{N_{tr}}\right)}{\left(1+\frac{\varepsilon\Gamma S}{V}\right)}$$

$$\rightarrow \bar{g} = \frac{\bar{g}_N ln\left(\frac{\bar{N}}{\bar{N}_{tr}}\right)}{(1+\bar{\varepsilon}S)}, \tag{20}$$

where $\bar{g}_N = \Gamma g_N$ is the effective differential gain coefficient, $\bar{N} = NV$ is the effective carrier number, $\bar{N}_{tr} = N_{tr}\ V$ is the effective transparent carrier number, and $\bar{\varepsilon} = \Gamma\varepsilon/V$ is the effective nonlinear gain saturation coefficient.

The values of $\bar{g}_N$, $\bar{N}_{tr}$, $\bar{\varepsilon}$, τ_n and τ_p can be extracted by the above steps. In the next step, the value ranges of the 1D

TWM parameters will be determined according to the values of the effective parameters, and the 1D TWM parameters will be extracted.

C. Parameter Extraction Based on 1D TWM

The effective parameters of the normalized rate equations derived in Section II.B will be plugged into the 1D TWM in this chapter, and the L-I curve and IM response will be fitted to separate the effective parameters and extract the 1D TWM parameters. The internal loss will be extracted at the same time. Because the normalized rate equations are the simplification of the 1D TWM, the value ranges of the effective parameters are modified to 0.5∼2 times to the extracted values. The values of the 1D TWM parameters (differential gain coefficient, transparent carrier density, nonlinear gain saturation coefficient and carrier lifetime) related to the effective parameters will be determined accordingly within these ranges. These determined value ranges are helpful to save the extraction time and ensure the fitting accuracy. Large-signal chirp fitting will be utilized to obtain the linewidth enhancement factor, and the effective index without injection will be modified by fitting the Bragg wavelength. When the temperature effect is ignored, the effective index drops as injected current increases. As a result, the effective index without injection extracted from the spectrum is lower than the actual value. The spectrum extraction value and the value plus 0.1 are set as the lower and higher limit of the no injection effective index, respectively. The linewidth enhancement factor's range is set to 1∼5, the internal loss's range is set to 0∼20/cm, and the optical confinement factor 's range is set to 0∼0.2. The following is the specific extraction method. Firstly, set initial values to effective index without injection, linewidth enhancement factor, internal loss, optical confinement factor and effective parameters of normalized rate equations according to their value ranges. Since the laser's structural parameters are known, the values of the other parameters of the 1D TWM will be determined correspondingly after the above initial values assigned. Secondly, the L-I curve, IM response and large-signal chirp are determined by using 1D TWM, and the Bragg wavelength is determined by using TMM. The error function of the aforesaid output results as well as the known results are then built. To identify the final values, the adaptive differential evolution algorithm is used to adjust the values of these parameters in order to discover the numerical minimizing of the error function.

The extraction of laser parameters based on 1D TWM has been finished at this stage. By fitting the output results, we can obtain laser's physical or quasi-physical parameters including grating coupling coefficient, effective index without injection, facet reflectivities, differential gain coefficient, transparent carrier density, nonlinear gain saturation coefficient, carrier lifetime, internal loss, linewidth enhancement factor and optical confinement factor.

III. Parameter Extraction Results

A. Parameter Extraction From Preset Simulation Results

In this Section, we preset a set of laser parameters and obtain the output characteristics by 1D TWM and TMM. Then, assuming the parameters are unknown, we extract the parameters by fitting the output results using the method presented in Section II.

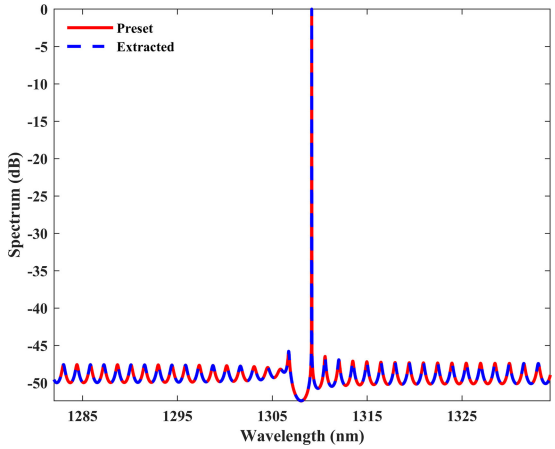

Fig. 1. Lasing spectra with preset parameters and extracted parameters. The "Preset" represents the simulation result with preset parameters and the "Extracted" represents the simulation result with extracted parameters.

TABLE I
Parameters of the DFB Laser Related to Spectrum

Name	Symbol (unit)	Preset value	Extracted value
Normalized grating coupling coefficient	κL	1.44	1.4287
Amplitude reflectivity of front facet	r_f	0.3	0.2962
Amplitude reflectivity of back facet	r_r	0.95	0.9497
Effective index without injection	n_{eff}^0	3.23	3.2285

1) Extraction Results Via Lasing Spectrum: By fitting the lasing spectrum as outlined in Section II.A, we first extract the grating coupling coefficient, effective index without injection, and facet reflectivities. Fig. 1 shows a comparison of the preset and the extracted spectra. During the extraction progress, linewidth enhancement factor is set to zero. Table I lists the preset parameters and the extracted parameters obtained by fitting the lasing spectrum. As evidenced by the result, the extracted parameters are quite close to the preset parameters and the spectrum derived from the extracted parameters agrees well with the preset spectrum.

2) Extraction Results of Normalized Rate Equations: The effective parameters of the laser are then extracted using the method outlined in Section II.B. According to the L-I curve, we can get a slope efficiency of 0.7091 mW/mA and a threshold current of 4.5 mA, as shown in Fig. 2. The relaxation oscillation frequencies and the quality factors corresponding to the IM response with the bias currents of 10 mA, 20 mA, and 30 mA are 8.8461 GHz/3.1695, 14.5925 GHz/2.1151 and 18.3551 GHz/1.7029. In Fig. 2(a) and (b), the preset results are compared with the analytical results. The analytical L-I curve is obtained using the slope efficiency and the threshold current, and the IM responses are analytically calculated by (15) using the quality factors and the relaxation oscillation frequencies. It can be seen

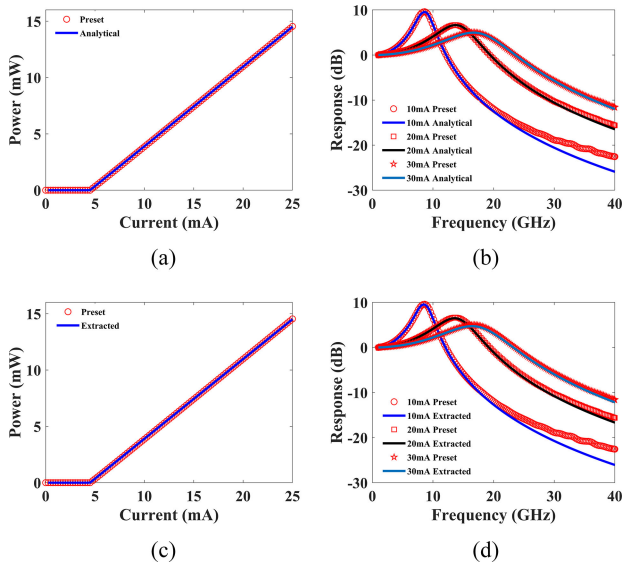

Fig. 2. L-I curve and IM response comparison diagram. (a) Simulated L-I curve with preset parameters by 1D TWM and analytical calculation L-I curve using the extracted slope efficiency and threshold current; (b) Simulated IM responses with preset parameters by 1D TWM and analytical calculation IM responses by (15) using the extracted quality factors and relaxation oscillation frequencies; (c) Simulated L-I curve with preset parameters by 1D TWM and simulated L-I curve with extracted effective parameters by (18), (19) and (20); (d) Simulated IM responses with preset parameters by 1D TWM and simulated IM responses with extracted effective parameters by (18), (19) and (20).

TABLE II
EFFECTIVE PARAMETERS OF NORMALIZED RATE EQUATIONS

Name	Symbol (unit)	Preset value	Extracted value
Effective differential gain coefficient	$\bar{g}_N\ (cm^{-1})$	160	123
Effective transparent carrier number	$\bar{N}_{tr}\ (10^7)$	1.04544	0.87
Effective nonlinear gain saturation coefficient	$\bar{\varepsilon}\ (10^{-7})$	1.8939	1.21
Carrier lifetime	$\tau_n\ (ns)$	0.5	0.4
Photon lifetime	$\tau_p\ (ps)$	2.5	3.5384

from the comparison results that the extracted slope efficiency, threshold current, relaxation oscillation frequencies and quality factors are accurate.

Table II lists the extracted parameters as well as the preset parameters, and Fig. 2(c) and (d) depict the extracted and the preset results. The preset photon lifetime is obtained by solving the eigenvalue equations of the quantum well DFB laser [30]. Although there are some differences between the extracted and the preset parameters, the overall trend of the extracted results is similar to the preset results. The results prove that the effective parameters derived from the slope efficiency, threshold current, relaxation oscillation frequencies and quality factors are accurate.

3) Extraction Results of 1D TWM: The effective parameters are separated by fitting the L-I curve and IM response, and the internal loss is extracted at the same time. Using large-signal chirp fitting, the linewidth enhancement factor is extracted, and

TABLE III
EXTRACTED PARAMETERS OF 1D TWM FROM PRESET RESULTS

Name	Symbol (unit)	Preset value	Extracted value
Optical confinement factor	Γ	0.1	0.1
Differential gain coefficient	$g_N(cm^{-1})$	1600	1750
Carrier lifetime	$\tau_n\ (ns)$	0.5	0.53918
Transparent carrier density	$N_{tr}\ (10^{18}cm^{-3})$	0.66	0.734
Nonlinear gain saturation coefficient	$\varepsilon\ (10^{-17}cm^3)$	3	3.1184
Internal loss	$\alpha\ (cm^{-1})$	10	10.0442
Effective index without injection	n_{eff}^0	3.23	3.2301
Linewidth enhancement factor	α_{LEF}	3	2.9528

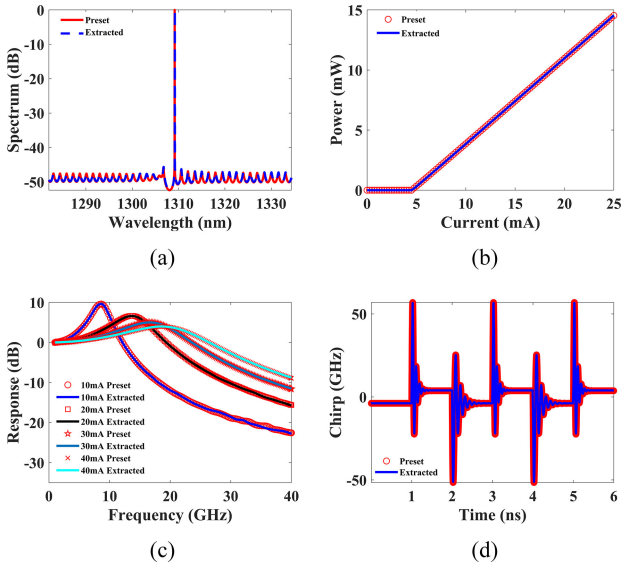

Fig. 3. (a) Lasing spectrum, (b) L-I curve, (c) IM response and (d) Large-signal chirp comparison diagram. The "Preset" represents the simulation results with preset parameters and the "Extracted" represents the simulation results with extracted parameters.

the effective index without injection is corrected by fitting the Bragg wavelength. Table III lists both the preset and the extracted parameters, and Fig. 3 shows the comparison of output characteristics. As can be seen from the results, the parameters we extracted are quite close to the preset parameters. The simulated laser output characteristics using the extracted parameters are quite similar to the preset output characteristics.

B. Parameter Extraction From Experimental Results

We apply the proposed method to extract parameters from the experimental results in this section. The measured lasing spectrum is used to determine the grating coupling coefficient, effective index without injection, and facet reflectivities. The values of the effective parameters of the normalized rate equations are extracted by the threshold current and slope efficiency of the L-I curve, as well as relaxation oscillation frequencies and

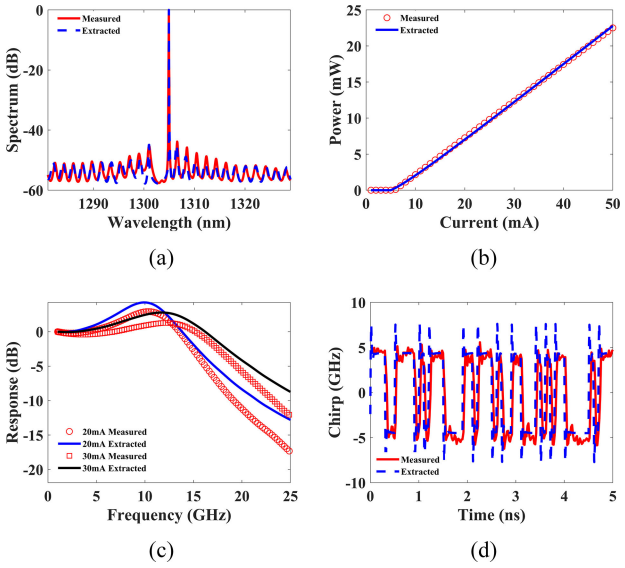

Fig. 4. (a) Lasing spectrum, (b) L-I curve, (c) IM response and (d) Large-signal chirp comparison diagram. The 'Measured' represents the experimental measured results and the "Extracted" represents the simulation results with extracted parameters.

quality factors of the IM response at various bias currents. Then the value ranges of the 1D TWM parameters are determined by the effective parameters, and the related 1D TWM parameters are extracted by fitting the L-I curve and IM response. The linewidth enhancement factor is extracted and the effective index without injection is modified by fitting large-signal chirp and Bragg wavelength. Fig. 4 shows a comparison of experimental and calculated results by using the extracted parameters. As shown, the calculated results with the extracted parameters by 1D TWM are in good agreement with the experimental results. The values of the extracted parameters are shown in Table IV.

IV. Conclusion

Based on 1D TWM, we propose a method for extracting the physical or quasi-physical parameters of the DFB laser from its output characteristics in this study. The effective index without injection, the grating coupling coefficient and the facet reflectivities are firstly extracted by fitting the lasing spectrum. The 1D TWM is then simplified to obtain the normalized rate equations and analytical formulae of effective parameters. The effective parameters in the normalized rate equations are extracted based on the L-I curve's threshold current and slope efficiency, as well as the relaxation oscillation frequencies and quality factors at various bias currents. After that, by fitting the L-I curve, IM response, large-signal chirp and Bragg wavelength, the effective parameters are separated and the 1D TWM parameters are extracted. The simulated results by using the extracted parameters are in good agreement with the preset results, despite the fact that there is minimal variance between the extracted parameters and the preset parameters. The method is also applied in experimental results extraction. The simulation results obtained by 1D TWM using the extracted parameters agree well with the experimental results, which further indicates the feasibility of this method. The 1D TWM-based parameter extraction approach can accurately reflect the physical features of the laser, making it a valuable tool for laser design, optimization and processing improvement.

TABLE IV
Extracted Parameters of 1D TWM From Experimental Results

Name	Symbol (unit)	Extracted value
Optical confinement factor	Γ	0.046
Grating coupling coefficient	$\kappa(cm^{-1})$	167
Differential gain coefficient	$g_N(cm^{-1})$	1746.5
Carrier lifetime	$\tau_n\ (ns)$	0.33
Transparent carrier density	$N_{tr}\ (10^{18}cm^{-3})$	0.62
Nonlinear gain saturation coefficient	$\varepsilon\ (10^{-17}cm^3)$	6.2
Internal loss	$\alpha\ (cm^{-1})$	12
Effective index without injection	n_{eff}^0	3.37
Linewidth enhancement factor	α_{LEF}	2.1
Amplitude reflectivity of front facet	r_f	0.1
Phase of front facet	φ_f	98.6°
Amplitude reflectivity of back facet	r_r	0.91
Phase of back facet	φ_r	177°
Cavity length	$L(\mu m)$	126
Active region volume	$V(\mu m^3)$	8.06
Grating period	$\Lambda(nm)$	193.43
Current injection efficiency	η	0.9

Appendix

The photon number rate equation is

$$\frac{dS}{dt} = \left(v_g \Gamma g - \frac{1}{\tau_p}\right) S + \gamma \Gamma v_g n_{sp} g. \tag{A1}$$

The carrier density rate equation is

$$\frac{dN}{dt} = \eta \frac{I}{eV} - \frac{N}{\tau_n} - \frac{\Gamma v_g g S}{V}. \tag{A2}$$

The material gain model for quantum well active region is

$$g = \frac{g_N ln\left(\frac{N}{N_{tr}}\right)}{\left(1 + \frac{\varepsilon \Gamma S}{V}\right)}. \tag{A3}$$

For small signal analysis, we have the following assumptions:

$$I(t) = I_0 + \Delta I(t),\ \Delta I(t) \ll I_0, \tag{A4-1}$$

$$S(t) = S_0 + \Delta S(t),\ \Delta S(t) \ll S_0, \tag{A4-2}$$

$$N(t) = N_0 + \Delta N(t),\ \Delta N(t) \ll N_0, \tag{A4-3}$$

where I_0, S_0, and N_0 are defined in the steady state solutions:

$$\left[v_g\Gamma g_0 - \frac{1}{\tau_p}\right] S_0 + \gamma n_{sp} v_g \Gamma\, g_0 = 0, \tag{A5-1}$$

$$g_0 = \frac{g_N ln\left(\frac{N_0}{N_{tr}}\right)}{1+\frac{\Gamma\varepsilon S_0}{V}}, \tag{A5-2}$$

$$\eta\frac{I_0}{eV} - \frac{N_0}{\tau_n} - \frac{v_g\Gamma g_0 S_0}{V} = 0. \tag{A5-3}$$

By utilizing (A5-1) to (A5-3) and ignoring higher order items, we have

$$\begin{aligned}\frac{d\Delta S}{dt} =& \left[v_g\Gamma\left(g_0 + \frac{\partial g}{\partial N}\Delta N + \frac{\partial g}{\partial S}\Delta S\right) - \frac{1}{\tau_p}\right](S_0+\Delta S)\\ &+ \gamma n_{sp} v_g\Gamma\left(g_0 + \frac{\partial g}{\partial N}\Delta N + \frac{\partial g}{\partial S}\Delta S\right)\\ \approx& \left[v_g\Gamma g_0 - \frac{1}{\tau_p} + v_g\Gamma\left(S_0+\gamma n_{sp}\right)\frac{\partial g}{\partial S}\right]\Delta S\\ &+ \left[v_g\Gamma\left(S_0+\gamma n_{sp}\right)\frac{\partial g}{\partial N}\right]\Delta N,\end{aligned} \tag{A6}$$

and from (A3) we have

$$\frac{\partial g}{\partial S} = \frac{g_N ln\left(\frac{N_0}{N_{tr}}\right)\left(-\frac{\Gamma\varepsilon}{V}\right)}{\left(1+\frac{\Gamma\varepsilon S_0}{V}\right)^2} = \frac{-\frac{\Gamma\varepsilon}{V}}{1+\frac{\Gamma\varepsilon S_0}{V}}\, g_0, \tag{A7-1}$$

$$\frac{\partial g}{\partial N} = \frac{g_N}{N_0\left(1+\frac{\Gamma\varepsilon S_0}{V}\right)} = \frac{g_0}{N_0 ln\left(\frac{N_0}{N_{tr}}\right)}. \tag{A7-2}$$

Similarly, we have

$$\begin{aligned}\frac{d\Delta N}{dt} =& \eta\frac{I_0+\Delta I}{eV} - \frac{1}{\tau_n}\left(N_0+\Delta N\right)\\ &- \frac{v_g\Gamma}{V}\left(g_0 + \frac{\partial g}{\partial N}\Delta N + \frac{\partial g}{\partial S}\Delta S\right)(S_0+\Delta S)\\ \approx& -\frac{v_g\Gamma}{V}\left(S_0\frac{\partial g}{\partial S} + g_0\right)\Delta S\\ &- \left(\frac{v_g\Gamma}{V}S_0\frac{\partial g}{\partial N} + \frac{1}{\tau_n}\right)\Delta N + \eta\frac{\Delta I}{eV}.\end{aligned} \tag{A8}$$

By defining

$$\begin{aligned}A' \equiv& -\left[v_g\Gamma g_0 - \frac{1}{\tau_p} + v_g\Gamma\left(S_0+\gamma n_{sp}\right)\frac{\partial g}{\partial S}\right]\\ \approx& v_g\Gamma g_0\frac{\frac{\Gamma\varepsilon S_0}{V}}{1+\frac{\Gamma\varepsilon S_0}{V}},\end{aligned} \tag{A9-1}$$

$$B' \equiv v_g\Gamma\left(S_0+\gamma n_{sp}\right)\frac{\partial g}{\partial N} \approx \frac{v_g\Gamma g_0}{N_0\ln\left(\frac{N_0}{N_{tr}}\right)}S_0, \tag{A9-2}$$

$$\begin{aligned}C' \equiv& \frac{v_g\Gamma}{V}\left(S_0\frac{\partial g}{\partial S} + g_0\right) = \frac{v_g\Gamma g_0}{V}\left(\frac{-\frac{\Gamma\varepsilon S_0}{V}}{1+\frac{\Gamma\varepsilon S_0}{V}} + 1\right)\\ =& \frac{v_g\Gamma g_0}{V}\frac{1}{1+\frac{\Gamma\varepsilon S_0}{V}},\end{aligned} \tag{A9-3}$$

$$D' \equiv \frac{v_g\Gamma}{V}S_0\frac{\partial g}{\partial N} + \frac{1}{\tau_n} = \frac{v_g\Gamma g_0}{N_0\ln\left(\frac{N_0}{N_{tr}}\right)}\frac{S_0}{V} + \frac{1}{\tau_n}, \tag{A9-4}$$

we can rewrite (A6) and (A8) as

$$\frac{d\Delta S}{dt} = -A'\Delta S + B'\Delta N, \tag{A10}$$

$$\frac{d\Delta N}{dt} = -C'\Delta S - D'\Delta N + \eta\frac{\Delta I}{eV}. \tag{A11}$$

By applying Fourier transform on (A10) and (A11), we obtain

$$\begin{aligned}H(\omega) =& \frac{\Delta S}{\Delta I}\\ =& \frac{\eta}{eV}\frac{B'}{(j\omega)^2 + j\omega\left(A'+D'\right) + \left(A'D'+B'C'\right)}\\ =& \frac{\eta B'}{eV}\frac{1}{(j\omega)^2 + (j\omega)\frac{\omega_r}{Q} + \omega_r^2},\end{aligned} \tag{A12}$$

$$S_{21} = \frac{H(\omega)}{H(0)} = \frac{\omega_r^2}{(j\omega)^2 + (j\omega)\frac{\omega_r}{Q} + \omega_r^2}. \tag{A13}$$

Here the relaxation oscillation frequency ω_r is defined as

$$\begin{aligned}\omega_r^2 =& A'D' + B'C'\\ =& v_g\Gamma g_0\frac{\frac{\Gamma\varepsilon S_0}{V}}{1+\frac{\Gamma\varepsilon S_0}{V}}\left[\frac{v_g\Gamma g_0}{N_0\ln\left(\frac{N_0}{N_{tr}}\right)}\frac{S_0}{V} + \frac{1}{\tau_n}\right]\\ &+ \frac{v_g\Gamma g_0}{V}\frac{S_0}{1+\frac{\Gamma\varepsilon S_0}{V}}\frac{v_g\Gamma g_0}{N_0\ln\left(\frac{N_0}{N_{tr}}\right)}\\ \approx& \frac{v_g S_0\Gamma g_N}{\tau_p V N_0}.\end{aligned} \tag{A14}$$

By utilizing (7), (12), and (14) in the paper, we can convert (A14) into

$$\begin{aligned}\omega_r =& \sqrt{\frac{2\lambda_0\Gamma L}{hcV}\frac{P_f}{\left(1-r_f^2\right)\tau_p}\frac{g_N}{N_0}}\\ =& \sqrt{\frac{\eta v_g\Gamma}{V}\frac{g_N}{N_{tr}e^{\frac{1}{v_g\Gamma g_N\tau_p}}}\frac{(I-I_{th})}{e}}.\end{aligned} \tag{A15}$$

The quality factor Q is defined in

$$\frac{\omega_r}{Q} = A' + D' \approx \frac{\Gamma\varepsilon S_0}{\tau_p V} + \frac{v_g\Gamma g_N}{N_0}\frac{S_0}{V} + \frac{1}{\tau_n}. \tag{A16}$$

By utilizing (7), (12), and (14) in the paper and (A14), we can convert (A16) into

$$\frac{1}{Q} = \frac{\varepsilon\omega_r}{v_g\frac{g_N}{N_{tr}e^{\frac{1}{v_g\Gamma g_N\tau_p}}}} + \tau_p\omega_r + \frac{1}{\tau_n\omega_r}. \tag{A17}$$

REFERENCES

[1] Y. Matsui et al., "112-Gb/s WDM link using two directly modulated Al-MQW BH DFB lasers at 56 Gb/s," in *Proc. Opt. Fiber Commun. Conf.*, 2015, Paper Th5B.6.

[2] T. Sudo et al., "Challenges and opportunities of directly modulated lasers in future data center and 5G networks," in *Proc. Opt. Fiber Commun. Conf.*, 2021, Paper Tu1B.3.

[3] K. Nakahara et al., "Direct modulation at 56 and 50 Gb/s of 1.3- μm InGaAlAs ridge-shaped-BH DFB lasers," *IEEE Photon. Technol. Lett.*, vol. 27, no. 5, pp. 534–536, Mar. 2015, doi: 10.1109/LPT.2014.2384520.

[4] Y. Matsui, "Directly modulated laser technology: Past, present, and future," in *Datacenter Connectivity Technologies: Principles and Practice.*, Aalborg, Denmark: River Publishers, 2017, pp. 87–172.

[5] S. Sulikhah, S. L. Lee, and H. W. Tsao, "Improvement on direct modulation responses and stability by partially corrugated gratings based DFB lasers with passive feedback," *IEEE Photon. J.*, vol. 13, no. 1, Feb. 2021, Art. no. 4900214, doi: 10.1109/JPHOT.2021.3056241.

[6] X. Li, *Optoelectronic Devices: Design, Modeling, and Simulation*. Cambridge, U.K.: Cambridge Univ. Press, 2009.

[7] G. P. Agrawal, *Fiber-Optic Communication Systems*, 4th ed., Hoboken, NJ, USA: Wiley, 2011.

[8] K. Petermann, *Laser Diode Modulation and Noise: K. Petermann*. Norwell, MA, USA: Kluwer Academic Publishers, 1988.

[9] G. P. Agrawal and N. K. Dutta, *Semiconductor Lasers: Govind P. Agrawal and Niloy K. Dutta*, 2nd ed. New York, NY, USA: Van Nostrand Reinhold, 2000.

[10] J. Park, X. Li, and W. P. Huang, "Comparative study of mixed frequency-time-domain models of semiconductor laser optical amplifiers," *IEE Proc.-Optoelectro.*, vol. 152, no. 3, pp. 151–159, 2005.

[11] J. Park, X. Li, and W.-P. Huang, "Performance simulation and design optimization of gain-clamped semiconductor optical amplifiers based on distributed Bragg reflectors," *IEEE J. Quantum Electron.*, vol. 39, no. 11, pp. 1415–1423, Nov. 2003, doi: 10.1109/JQE.2003.818287.

[12] M. J. Connelly, "Wideband semiconductor optical amplifier steady-state numerical model," *IEEE J. Quantum Electron.*, vol. 37, no. 3, pp. 439–447, Mar. 2001, doi: 10.1109/3.910455.

[13] D. J. Jones, L. M. Zhang, J. E. Carroll, and D. D. Marcenac, "Dynamics of monolithic passively mode-locked semiconductor lasers," *IEEE J. Quantum Electron.*, vol. 31, no. 6, pp. 1051–1058, Jun. 1995, doi: 10.1109/3.387042.

[14] J. C. Cartledge and R. C. Srinivasan, "Extraction of DFB laser rate equation parameters for system simulation purposes," *J. Lightw. Technol.*, vol. 15, no. 5, pp. 852–860, May 1997, doi: 10.1109/50.580827.

[15] H. M. Salgado, J. M. Ferreira, and J. J. O'Reilly, "Extraction of semiconductor intrinsic laser parameters by intermodulation distortion analysis," *IEEE Photon. Technol. Lett.*, vol. 9, no. 10, pp. 1331–1333, Oct. 1997, doi: 10.1109/68.623253.

[16] H. Yasaka, K. Takahata, and M. Naganuma, "Measurement of gain saturation coefficients in strained-layer multiple quantum-well distributed feedback lasers," *IEEE J. Quantum Electron.*, vol. 28, no. 5, pp. 1294–1304, May 1992, doi: 10.1109/3.135269.

[17] L. Bjerkan, A. Royset, L. Hafskjaer, and D. Myhre, "Measurement of laser parameters for simulation of high-speed fiberoptic systems," *J. Lightw. Technol.*, vol. 14, no. 5, pp. 839–850, May 1996, doi: 10.1109/50.495166.

[18] P. Pérez, A. Valle, I. Noriega, and L. Pesquera, "Measurement of the intrinsic parameters of single-mode VCSELs," *J. Lightw. Technol.*, vol. 32, no. 8, pp. 1601–1607, Apr. 2014, doi: 10.1109/JLT.2014.2308303.

[19] D. Hofstetter and R. L. Thornton, "Measurement of the Q factor of semiconductor laser cavities by Fourier analysis of the emission spectrum," in *Proc. Fabr. Testing Rel. Appl. Semicond. Lasers III*, 1998, pp. 66–77.

[20] I. Fatadin, D. Ives, and M. Wicks, "Numerical simulation of intensity and phase noise from extracted parameters for CW DFB lasers," *IEEE J. Quantum Electron.*, vol. 42, no. 9, pp. 934–941, Sep. 2006, doi: 10.1109/JQE.2006.880117.

[21] Z. Ma, P. Feng, and Y. Li, "Inverse design of semiconductor laser parameters based on deep learning and particle swarm optimization method," in *Proc. 11th Int. Conf. Inf. Opt. Photon.*, 2019, Art. no. 112092X.

[22] Z. Ma and Y. Li, "Parameter extraction and inverse design of semiconductor lasers based on the deep learning and particle swarm optimization method," *Opt. Exp.*, vol. 28, no. 15, pp. 21971–21981, 2020, doi: 10.1364/OE.389474.

[23] R. Schatz, E. Berglind, and L. Gillner, "Parameter extraction from DFB lasers by means of a simple expression for the spontaneous emission spectrum," *IEEE Photon. Technol. Lett.*, vol. 6, no. 10, pp. 1182–1184, Oct. 1994, doi: 10.1109/68.329632.

[24] T. Makino and J. Glinski, "Transfer matrix analysis of the amplified spontaneous emission of DFB semiconductor laser amplifiers," *IEEE J. Quantum Electron.*, vol. 24, no. 8, pp. 1507–1518, Aug. 1988, doi: 10.1109/3.7077.

[25] M. Yamada and K. Sakuda, "Analysis of almost-periodic distributed feedback slab waveguides via a fundamental matrix approach," *Appl. Opt.*, vol. 26, no. 16, pp. 3474–3478, 1987, doi: 10.1364/AO.26.003474.

[26] Y.-C. Lin, F.-S. Wang, and K.-S. Hwang, "A hybrid method of evolutionary algorithms for mixed-integer nonlinear optimization problems," in *Proc. Congr. Evol. Computation-CEC99*, 1999, vol. 3, pp. 2159–2166.

[27] D. K. Tasoulis, N. G. Pavlidis, V. P. Plagianakos, and M. N. Vrahatis, "Parallel differential evolution," in *Proc. Congr. Evol. Computation*, 2004, vol. 2, pp. 2023–2029.

[28] U.-C. Lin, K.-S. Hwang, and F.-S. Wang, "Plant scheduling and planning using mixed-integer hybrid differential evolution with multiplier updating," in *Proc. Congr. Evol. Computation*, 2000, vol. 1, pp. 593–600.

[29] Y. Xi, X. Li, and W.-P. Huang, "Time-domain standing-wave approach based on cold cavity modes for simulation of DFB lasers," *IEEE J. Quantum Electron.*, vol. 44, no. 10, pp. 931–937, Oct. 2008, doi: 10.1109/JQE.2008.2000922.

[30] Y. Xi, W.-P. Huang, and X. Li, "An efficient solution to the standing-wave approach based on cold cavity modes for simulation of DFB lasers," *J. Lightw. Technol.*, vol. 27, no. 15, pp. 3227–3234, Aug. 2009, doi: 10.1109/JLT.2008.2010335.